Polymer 56 (2015) 464–475

Contents lists available at ScienceDirect

Polymer

journal homepage: www.elsevier.com/locate/polymer

Cellulose nanocrystal/polyolefin biocomposites prepared by solid-state shear pulverization: Superior dispersion leading to synergistic property enhancements

Krishnan A. Iyer [a], Gregory T. Schueneman [b], John M. Torkelson [a, c, *]

[a] Department of Chemical and Biological Engineering, Northwestern University, Evanston, IL 60208, USA
[b] Forest Products Laboratory, U.S. Forest Service, Madison, WI 53705, USA
[c] Department of Materials Science and Engineering, Northwestern University, Evanston, IL 60208, USA

ARTICLE INFO

Article history:
Received 12 October 2014
Received in revised form
4 November 2014
Accepted 9 November 2014
Available online 14 November 2014

Keywords:
Cellulose nanocrystals
Composites
Polyolefins

ABSTRACT

Cellulose nanocrystals (CNCs), a class of renewable bionanomaterials with excellent mechanical properties, have gained major interest as filler for polymers. However, challenges associated with effective CNC dispersion have hindered the production of composites with desired property enhancements. Here, composites of polypropylene (PP) and low density polyethylene (LDPE) with 5–10 wt% unmodified CNC are produced for the first time via a solventless process. In particular, we employ solid-state shear pulverization (SSSP). Optical and electron microscopy reveals excellent CNC dispersion with strongly suppressed degradation relative to composites made by melt mixing. Effective dispersion leads to major increases in Young's modulus, including a 69% increase in 90/10 wt% LDPE/CNC composites relative to neat LDPE, the highest modulus enhancement ever reported for polyolefin/CNC composites. The composites also exhibit superior creep performance with modest increment in yield strength compared to neat polymer. The LDPE/CNC composites retain elongation at break values that are equal to that of neat polymer while a decrease is observed with PP/CNC composites. The CNC thermal degradation temperature in air is close to that of PP melt processing conditions. We hypothesize that during melt-processing CNCs undergo preferential thermo-oxidative degradation in LDPE and simultaneous degradation in PP. Thus, CNC incorporation results in impaired thermal stability in LDPE and, especially, PP. Care must be taken in selecting the post-SSSP melt processing temperature and residence time in order to suppress degradation. Taking that into account, this study has produced polyolefin/CNC composites with superior dispersion and property enhancements and shown that CNC is an attractive filler for green polymer biocomposites.

1. Introduction

In comparison to composites with micron-scale fillers (e.g., glass, carbon black, mineral fillers, etc. [1–7]), polymer nanocomposites exhibit property enhancements at much lower filler loadings and thus have gained widespread interest. Ever since the pioneering work two decades ago on polymer/layered silicate composites by Toyota researchers [8], a wide range of nanofillers such as carbon nanotubes, expanded graphite, graphene, silica and calcium carbonate have been investigated in depth [9–25]. In addition, growing interest in developing a greener polymer industry has prompted researchers to explore green polymer composites [26], leading to the emergence of studies incorporating lignocellulosic materials such as rice husk, natural fiber and sawdust as fillers for plastics [27–35]. Detailed reviews of work on green polymer composites can be found in Refs. [36–39]. Besides cellulose-based natural fillers, several studies of composites with pure forms of cellulose such as microcrystalline cellulose have also been reported in depth [40–42]. In the current study, we investigate the potential of using cellulose nanocrystals as green nanofillers for the preparation of synergistic polymer composites.

* Corresponding author. Department of Chemical and Biological Engineering, Northwestern University, Evanston, IL 60208, USA.
E-mail address: j-torkelson@northwestern.edu (J.M. Torkelson).

http://dx.doi.org/10.1016/j.polymer.2014.11.017
0032-3861/

1.1. Brief background on cellulose nanocrystals and strategies for producing polymer composites

Individual cellulose crystallites known as cellulose nanocrystals that form the building blocks for cellulose structures in plants have attracted major interest recently as a green nanoreinforcing agent in polymer matrix composites (PMCs). The existence of such nanocrystallites was demonstrated as early as the 1950's [43,44]. Although such nanocrystals are known by several names such as nanofibrils, nanocellulose, and nanowhiskers, the Textile Association of Pulp and Paper Industry has proposed cellulose nanocrystals (CNCs) as the standard nomenclature. Cellulose nanocrystals can be conveniently extracted from bulk cellulose by mechanical or chemical treatment to separate out the crystalline phases. Commonly employed techniques include acid hydrolysis [45,46], TEMPO-mediated oxidation [47,48], and homogenization and grinding [49,50]. In addition to biorenewability, the extracted CNCs possess attractive properties including high modulus on par with Kevlar™ [51–53], uniform prismatic dimensions [51–53], low coefficient of thermal expansion [54], lyoprotic liquid crystallinity [51–53], easy orientability under shear [54,55], refractive index on par with most polymers [56], high piezoelectric constants [57] and large surface area (~100 m^2/g [51–53]). Pilot-scale plants for the production of CNCs are already operational with capacities up to 25 kg/batch [58,59]. It is estimated that the annual world-wide production of CNCs will increase by up to 500% by 2017, providing an abundant supply for the production of composites [53]. Large-scale production of CNCs is expected to reduce their overall cost, making them less costly than other nanomaterials like carbon nanotubes [60]. These attractive traits make CNCs highly desirable fillers.

The first efforts to produce PMCs with CNC date to the 1990s [61]. However, achieving homogenous dispersion of CNC in the host polymer matrix has been a major challenge. The hydrophilic nature of CNC and the large interfacial attraction due to its nanoscale dimensions result in significant filler agglomeration during processing, thereby dramatically impairing the ability of CNCs to act as nanoscale reinforcements for polymers [51–53,62,63]. Common strategies used to produce PMCs with CNCs are described in the following paragraphs.

A commonly employed strategy involves producing a stable colloidal dispersion of CNC in aqueous media. The presence of pendant sulfate groups left from acid hydrolysis steps during CNC production aids the formation of such dispersions. As a result, several studies have employed water-soluble polymers or polymer latex for making such composites [51–53,62–64]. Favier et al. [61] demonstrated for the first time the incorporation of CNC through emulsion polymerization with styrene/butadiene rubber. Composites of water-soluble polymers such as poly(vinyl alcohol) and poly(ethylene oxide) (PEO) have shown improvements in mechanical and barrier properties [65–67]. Recent studies have also produced water-based epoxy, elastomeric nanocomposites, and hydrogels incorporating CNCs [68–71].

Other studies have produced PMCs by employing surfactant-modified CNC to achieve good dispersion in aprotic solvents such as toluene [72–74]. However, relatively few studies have attempted to produce composites of polyolefins with cellulose nanocrystals due to solubility limitations. Ljungberg et al. [75] employed pristine and surfactant-modified cellulose whiskers in hot toluene to produce solvent-cast composite films with polypropylene (PP). Such composites with 6 wt% unmodified cellulosic whiskers showed impaired mechanical properties with brittle fracture and elongation values that were only 50% of strain at yield of neat PP. Agarwal et al. [76] dissolved maleic anhydride-grafted PP/CNC mixtures in toluene. Upon solvent evaporation, the resulting powder was milled and blended in a lab-scale extruder into filaments. Because of poor dispersion, the modulus of the PP composite with 2 wt% CNC was only 17% higher than that of neat PP. Bahar et al. [77] employed ultrasonication to disperse pristine cellulose nanowhiskers in toluene. This dispersion was then used to produce composites with neat PP employing maleic anhydride-grafted PP (MAPP) as compatibilizer under strong magnetic stirring. Such composites with 10 wt% cellulose nanowhisker and 2 wt% MAPP exhibited a 20% reduction in Young's modulus with respect to neat PP. Besides resulting in ineffective dispersion, such solvent-based techniques are unlikely to be adopted commercially because they are both expensive and environmentally unfriendly.

Relatively few studies have produced polyolefin/CNC composites by industrial processing techniques such as melt extrusion. The inability of melt mixing to provide sufficiently large shear stresses to break up and disperse CNCs results in large CNC agglomerates within the polymer [53]. Moreover, the presence of sulfate groups in CNCs leads to inferior thermal stability with degradation temperatures close to 150 °C [78,79]. Thus, attempts at achieving filler dispersion in polyolefins via melt extrusion, which employs long mixing times, and high temperature (~200 °C for PP and poly(lactic acid) (PLA)) is often accompanied by major filler degradation [79–82]. Studies have investigated different strategies to prevent CNC degradation. For instance, end-group functionalized CNC with organic acid chloride [82] or CNC grafted with poly(caprolactone) [80], poly(vinyl alcohol) [83], or PLA [81] have been extruded with polyolefins. Cellulose nanocrystals wrapped with PEO or high molecular weight polyamides have also been used to produce composites via melt extrusion [84–88]. Recently, Oksman and coworkers have employed a liquid feeding technique for producing composites of PLA and a colloidal dispersion of CNC via melt extrusion [81,83].

To prevent CNC degradation, researchers have chosen low-melting-point polyolefins such as low density polyethylene (LDPE) as matrix polymers [82]. Dufresne and coworkers [82] produced composites with pristine CNC and CNC functionalized with long chain organic chlorides. Such LDPE/pristine CNC composites with 10 wt% filler exhibited 25 and 85% reductions in tensile strength and elongation at break, respectively, with only a 24% increase in Young's modulus. On the other hand, CNC functionalization impaired the modulus and tensile strength of the composites. In another study by Dufresne and coworkers [87], water soluble PEO was blended with equal masses of aqueous CNC dispersions, freeze dried, and then melt blended with LDPE. When 9 wt% 1.0×10^6 g/mol PEO-wrapped-CNC was incorporated into LDPE, the resulting composite exhibited a 60% increase in modulus and maintained the elongation to break value of neat LDPE [87]. All strategies discussed above involve either additional chemistry, which reduces the green aspect of the CNCs and adds cost, or employ hygroscopic compatibilizers or surfactants that add processing steps and cost. Thus, there is a need for a simple, industrially scalable, green strategy for producing polyolefin composites with well-dispersed CNCs.

1.2. Solid-state shear pulverization: A new strategy for producing polyolefin/CNC composite materials

Here, we employ a single-step, solventless, continuous and industrially scalable process called solid-state shear pulverization (SSSP) [14,15,19,89–103] to produce green composites of polyolefins and CNCs with excellent dispersion and remarkable property enhancements compared to those reported in literature. (The SSSP process is one of a class of solid-state processing methods including mechanical milling techniques such as ball and pan milling that have been used in studies of polymer composites and

nanocomposites [90,104–111]. It is noteworthy that no previously reported study involving solid-state processing has employed CNC as filler. Unlike the other solid-state methods, SSSP is a continuous processing technique.) Although the current study uses a lab-scale apparatus, polyolefins have been processed at throughputs exceeding 150 kg/h with a commercial-scale apparatus at Northwestern University [99,100]. The SSSP process employs a modified twin-screw extruder in which materials are cooled rather than heated, so that the polymer is processed below its glass transition temperature if amorphous or below its melt temperature if semi-crystalline. Solid-state processing exposes the polymers to larger shear and compressive forces than those normally encountered in twin-screw melt extrusion. Mechanical energy stored during SSSP brings about material fracture or fragmentation followed by random fusion, which is repeated many times during the average residence time of the materials within the pulverizer.

The solid-state material and near-ambient-temperature process conditions in SSSP facilitate intimate mixing between polymer and nanofiller and eliminate the common limitations of thermodynamics, viscosity mismatch, and filler degradation associated with melt processing [96,99,100]. Past studies have demonstrated the ability of SSSP to produce well-dispersed polymer nanocomposites with fillers ranging from layered structures, e.g., clay and graphite, to bundled carbon nanotubes [14,15,17,19,89,90]. Blend compatibilization with dispersed-phase size approaching 100 nm has been achieved through SSSP processing [91,92]. The formation of trace levels of block copolymer at the polymer blend interface resulting from recombination of polymer radicals has been reported as the driving force for in situ, immiscible blend compatibilization through SSSP [93–95]. Green PMCs with starch, rice husk ash, and eggshell filler have been produced with SSSP [97–100]. Taking advantage of the near-ambient-temperature processing, SSSP was very recently used to functionalize PP with maleic anhydride or ester moieties without significant reduction in PP molecular weight, thereby overcoming a limitation associated with commercial melt-state processes to achieve such grafting [101,102].

The current study explores the potential of SSSP as an effective tool for producing synergistic polyolefin/CNC biocomposites with unmodified CNC. The near-ambient-temperature, solid-state processing nature of SSSP helps to overcome the twin challenges of filler dispersion and filler degradation associated with melt processing of polymer/CNC biocomposites. Superior dispersion and suppression of degradation of CNC filler in polyolefins are demonstrated via optical and electron microscopy. Major property enhancements in tensile, creep and crystallization behavior of the biocomposites are quantified and compared to literature values. Finally, the thermal stability of the resulting biocomposite materials is ascertained by thermogravimetric analysis in nitrogen and air atmospheres, which is important in considering the viability or limitations of melt processing such materials into final products.

2. Experimental

2.1. Materials

Two polypropylene samples with density of 0.905 g/cm^3 and melt flow indexes (MFIs) of 2 g/10 min and 9 g/10 min (230 °C and 2.2 kg load), respectively, were obtained from Total Petrochemicals. Low density polyethylene with density of 0.919 g/cm^3 and MFI of 1.1 g/10 min (190 °C and 2.2 kg load) was supplied by ExxonMobil.

2.2. Preparation of cellulose nanocrystals

Cellulose nanocrystals were produced at Forest Products Laboratory in Madison, WI as described in Ref. [58]. In brief, the lab-scale procedure described by Beck-Candanedo et al. [46] is scaled up to produce 25 kg of CNC per batch. 50 kg of machine-dried pre-hydrolysis Kraft rayon grade dissolving wood pulp is cut into 0.6 × 0.4 cm strips and placed in a 400 L glass-lined vessel. Preheated sulfuric acid (64% by weight) is then added to the pulp under an inert nitrogen atmosphere, and the temperature of the mixture is increased to 45 °C. After 90 min, the degraded pulp is transferred to a 6000 L reactor and diluted with ~3000 L of water. Color is removed by adding hypochlorite solution and acid neutralization by sodium hydroxide. After settling of reaction products, the leftover salt/sugar solution is removed. Purification is completed by salt removal and filtration, bringing the final concentration to 6–10 wt%, which is a 50% yield.

Water is removed from the CNC aqueous dispersion by freeze-drying. In this procedure, 9 wt% *t*-butanol is added to suppress freezing, and the dispersion is passed through a Taylormate Shakemaster (model 450-12) to pre-chill it to −3 °C in ~5 min. The chilled dispersion is then placed in trays, and freezing is completed at −20 °C. The freeze-drying is accomplished in a Vertis GPFD-36Dx66-35XL freeze drier under vacuum of at least 50 mTorr at 45 °C.

2.3. Preparation of polyolefin/CNC composites

Polyolefin pellets (LDPE pellet or 2 g/10 min MFI PP pellet) were fed to a Berstorff ZE-25 pulverizer with a K-tron S-60 feeder at a feed rate of 90 g/h. The CNC was added to the pulverizer using a powder feeder (Brabender Technologies Inc. DDSR 12-1 volumetric feeder) at different feed rates depending on the desired filler content in the final composite. The polyolefin pellets and CNC were pulverized with a screw speed of 200 RPM. The pulverizer barrels were cooled by a recirculating ethylene glycol/water mix at −7 °C (Budzar Industries WC-3 chiller). The pulverizer has a 25-mm-diameter section containing spiral conveying and bilobe kneading elements (mixing) that provide intimate mixing between the polyolefin pellets and CNC powder. Following this is a small section where the barrel diameter transitions from 25 to 23 mm. (It should be noted that SSSP can be run with all sections having a 25-mm-diameter barrel.) The bulk of the pulverization and filler dispersion take place in the final 23-mm-diameter section of the pulverizer barrel, which contains trilobe shearing elements. With the mixing zone containing one reverse, two neutral, and three forward kneading elements and the pulverization zone containing three forward, two neutral, and two reverse shearing elements, the screws employed here were designed to impart high specific energy to the material [103].

Fine powder of polyolefin/CNC composites with 5–10 wt% CNC was prepared with SSSP as described above. For comparison, 90/10 wt% PP/CNC and LDPE/CNC composites were produced by melt mixing (MM) for 10 min at 180 °C and 140 °C, respectively, with an ATLAS Electronics Devices MiniMax molder (cup-and-rotor mixer) at rotor speed of 160 RPM. Three steel balls were added to induce chaotic mixing [112].

In addition, to understand thermal degradation during melt processing, composites of PP and 5 wt% CNC were prepared via SSSP. High MFI index (9 g/10 min) PP was used for this part of the study, in order that the composite material possesses sufficiently low viscosity at the low melt extrusion temperatures used here. The fine-powder SSSP output was fed to a single-screw melt extruder (Randcastle RCP-0625 microtuder) which was operated with a 50 RPM screw speed and 175–220 °C zone temperatures.

2.4. Characterization of polyolefin/CNC composites

Optical micrographs of compression-molded films of 0.7 mm thickness were taken using a Heerburg Wild M3Z stereoscope. Field

emission-scanning electron microscopy (FE-SEM) samples were prepared for PP/CNC and LDPE/CNC composites by melting and extruding at 180 °C or 140 °C, respectively, using a MiniMax molder. The morphologies of the cryofractured sections of composites were obtained using a Hitachi SU 8030 FE-SEM after sputter coating (Denton Desk III) with gold. The morphology of pristine CNC was obtained after solution casting from an aqueous dispersion.

Uniaxial tensile testing samples were prepared by compression molding the SSSP powder in a PHI (model 0230 C-X1) press at 180 °C and 140 °C for PP and LDPE, respectively, for 5 min with a 5 ton ram force followed by immediate cooling in a cold press at 10 °C under 5 ton ram force. Tensile coupons were cut using a standard Dewes-Gumbs dogbone die. Samples were equilibrated at room temperature for 48 h and then tested (ASTM D1708) using an MTS Sintech 2S tensile tester equipped with a 5 kN load cell at a cross head speed of 50 mm/min. Five samples were tested for each composite and the results averaged to obtain a mean value. Short-term creep measurements at room temperature were performed with an MTS 810 instrument on dogbone samples similar to those used for tensile testing. Creep tests were performed at a stress of 50% of the yield strength value measured from tensile test data for a total of 3600 s.

Crystallization of PP and LDPE in the composites and the neat state were characterized using a Mettler Toledo 822e differential scanning calorimeter (DSC). After annealing at 180 °C, samples were cooled at 10 °C/min to determine the non-isothermal crystallization onset temperature of polyolefin in the composite. To calculate crystallinity of the polymer in the composite, the specific enthalpy derived from the area associated with the crystallization portion of the nonisothermal cooling curve was divided by the mass fraction of the polymer in the composite; this value was subsequently divided by the theoretical heat of fusion for PE and PP of 285.9 and 207.1 J/g, respectively [113,114]. Isothermal crystallization half-times for PP/CNC composites were determined at 140 °C after cooling at a rate of 40 °C/min from 180 °C.

Thermal degradation behavior was monitored using a thermogravimetric analyzer (Mettler Toledo 851e) calibrated with an indium/aluminum standard. Neat polymer and composite samples were heated to 700 °C using a 10 °C/min heating ramp in both N_2 and air environment to determine thermal and thermoxidative degradation behavior.

3. Results and discussion

3.1. Dispersion of CNC in polyolefin/CNC composites

Fig. 1 compares the appearance of compression-molded films of 90/10 wt% PP/CNC and LDPE/CNC composites that are produced by SSSP and by MM (using a MiniMax molder). Melt mixing of pristine CNC into LDPE at 140 °C and into PP at 180 °C (Fig. 1a and b) results in inhomogeneous filler dispersion within the polymer matrix. The hydrophilic nature of cellulose particles and failure of melt mixing to provide sufficiently large shear forces lead to significant agglomeration, with agglomerates approaching 1 mm in size that are visible to the naked eye in both polymer matrices. For instance, the PP/CNC composite produced by MM has a brownish color with black dots throughout the matrix. Major degradation of CNC within the polymer matrix is caused by the inferior thermal stability of cellulose, which is further impaired by the 150 °C degradation temperature of the sulfate end groups left from the acid hydrolysis step during its preparation [78,79]. In contrast, 90/10 wt% LDPE/CNC and PP/CNC composites produced via SSSP (and subsequently compression molded into films at 140 °C and 180 °C, respectively) exhibit a uniform tan color with no visible particle agglomerates (Fig. 1c and d). This is due to the large forces and stresses provided by the solid-state processing nature of SSSP that can break up and disperse particles effectively. Besides excellent dispersion, the near-ambient-temperature conditions employed in SSSP prevent filler degradation at that stage.

As discussed above, in addition to particle agglomeration, the long mixing times and high temperatures employed in conventional melt processing such as twin-screw extrusion (TSE) often cause major CNC degradation. Dufresne and coworkers attempted several strategies to improve dispersion and suppress CNC degradation in LDPE and polystyrene (PS) [82,86,87]. In their study [82], LDPE/CNC composites with up to 10 wt% pristine CNC produced via TSE at 160 °C showed inhomogeneous filler dispersion with dark dots of degraded CNC, similar to the composite samples produced by MM in this study. Further grafting of CNC with organic acid chloride or addition of PEO compatibilizer [87] helped to improve dispersion and reduce degradation. In another study by Lin et al. [86], PS was extruded at 200 °C with pristine CNC, CNC grafted with short chain poly(ethylene glycol) (CNC-g-PEG), and CNC-g-PEG wrapped with PEO. Such composites with 8 wt% pristine CNC filler presented the same degradation issues as discussed above. Despite the chemistry, composites made with modified CNC fillers exhibited significant filler agglomeration with particles visible to the naked eye as shown in the micrographs provided in their study. In our study, SSSP production of LDPE and PP composites with pristine CNC manages to suppress filler degradation with no visible particle agglomeration. In short, SSSP shows significant promise in producing well-dispersed polyolefin/CNC composite materials without degradation, thereby eliminating the need for performing additional chemistry and improving the green value of the final composite.

Fig. 2a shows a typical FE-SEM image of as-received CNC. The micrograph shows 50–100 μm particles and agglomerates, which are a result of strong interparticle attraction due to the hydrophilic

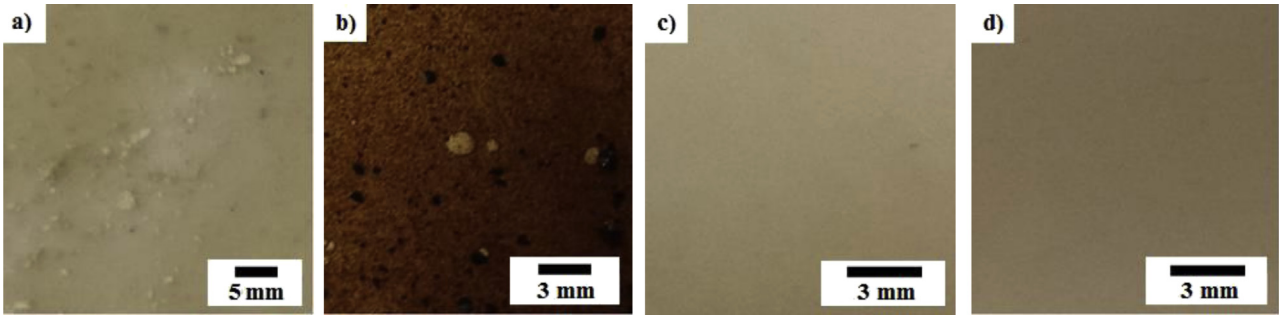

Fig. 1. Optical micrographs of a) 90/10 wt% LDPE/CNC (MM), b) 90/10 wt% PP/CNC (MM), c) 90/10 wt% LDPE/CNC (SSSP) and d) 90/10 wt% PP/CNC (SSSP).

nature of CNCs. This hydrophilic nature has been cited as a main reason for the difficulty in achieving good CNC dispersion via conventional melt processing [82].

FE-SEM images of cryofractured cross sections of LDPE/CNC and PP/CNC composites produced by MM and SSSP are shown in Fig. 2b–f. The micrographs support the conclusions drawn from the optical micrographs about CNC dispersion within the composites. Severe particle agglomeration is observed in melt-mixed composites with particles approaching 50–100 μm in both LDPE and PP composites (Fig. 2 b and c). Thus, MM provides little to no CNC dispersion within the polyolefin matrix. In contrast, SSSP-processed composites (Fig. 2 d and e) show excellent dispersion with CNC particles wetted into the polymer matrix and with particle sizes less than 2 μm. Furthermore, Fig. 2f and g reveal major agglomerate size reduction achieved by SSSP, with needle-like single CNC particles that are only a few nanometers in diameter and a few hundred nanometers in length. It is noteworthy that wood cellulose nanocrystals similar to those employed in this study typically have a diameter of 3–5 nm and a length of 300–400 nm [46]. Therefore, the nanometer-sized particles observed in the micrographs have demonstrated the ability of SSSP processing to break up CNC agglomerates to individual nanocrystals in the matrices. In brief, both optical and electron micrographs indicate that SSSP yields excellent CNC dispersion in polyolefin matrices with suppressed degradation.

3.1.1. Mechanical properties of polyolefin/CNC composites – tensile

Tables 1 and 2 summarize the effect of CNC incorporation on the mechanical properties of LDPE/CNC and PP/CNC composite materials produced by SSSP and MM. (It must be noted that the mechanical test samples were produced by melt-state compression molding of composite materials made by SSSP or MM.) Incorporation of CNC into LDPE by SSSP gives rise to a monotonic increase in Young's modulus with increasing CNC content. For instance, there is a 38% increase over neat LDPE with 5 wt% CNC content and a 69% increase with 10 wt% CNC content. Similarly, PP/CNC composites prepared by SSSP exhibit a 40% increase in Young's modulus over neat PP with 5 wt% CNC and a 53% increase with 10 wt% CNC content. Relative to neat polymer, SSSP-processed composites show maximum ~30% and ~8% increases in yield strength for LDPE/CNC and PP/CNC composites, respectively.

Table 1
Tensile properties of LDPE/CNC composites.

Specimen	Processing method	Young's modulus E (MPa)	Yield strength σ_y (MPa)	Elongation at break ε_B (%)
Neat LDPE	–	160 ± 10	10 ± 1	510 ± 30
95/5 wt% LDPE/CNC	SSSP	220 ± 10	11 ± 1	490 ± 30
93/7 wt% LDPE/CNC	SSSP	250 ± 10	12 ± 1	500 ± 40
90/10 wt% LDPE/CNC	SSSP	270 ± 10	13 ± 1	460 ± 30
90/10 wt% LDPE/CNC	MM	180 ± 20	7 ± 1	20 ± 10

Table 2
Tensile properties of PP/CNC composites.

Specimen	Processing method	Young's modulus E (MPa)	Yield strength σ_y (MPa)	Elongation at break ε_B (%)
Neat PP	–	1200 ± 20	36 ± 1	700 ± 40
95/5 wt% PP/CNC	SSSP	1680 ± 50	39 ± 1	15 ± 2
93/7 wt% PP/CNC	SSSP	1730 ± 60	39 ± 1	13 ± 2
90/10 wt% PP/CNC	SSSP	1830 ± 70	38 ± 1	12 ± 3
90/10 wt% PP/CNC	MM	1480 ± 50	34 ± 1	7 ± 2

Tables 1 and 2 also provide mechanical test results for 10 wt% CNC in LDPE and PP matrices prepared by MM. The melt-mixed LDPE/CNC composites exhibit a 13% increase in Young's modulus relative to that of neat LDPE, and PP/CNC composites show a 23% increase. Composites of LDPE and PP with same filler content prepared by SSSP are 50% and 24% stiffer than their MM counterparts. In addition, PP/CNC composites prepared by MM have similar yield strength as neat polymer, while LDPE/CNC composites show a 30% decrease. These results are consistent with superior dispersion achieved by SSSP and little to no thermal degradation during post-

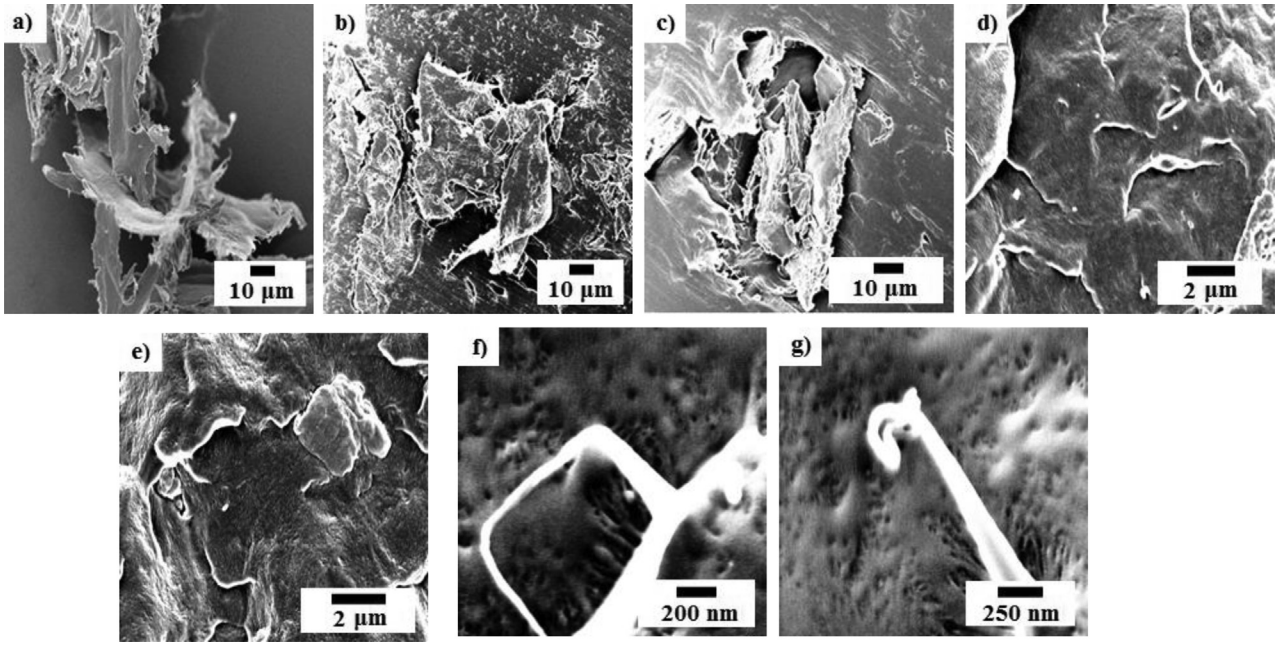

Fig. 2. FE-SEM images of a) as-received CNC, b) 90/10 wt% LDPE/CNC (MM), c) 90/10 wt% PP/CNC (MM), d) 90/10 wt% LDPE/CNC (SSSP), e) 90/10 wt% PP/CNC (SSSP), f) magnified FE-SEM image of d) showing individual CNCs in LDPE, and g) magnified image of e) showing individual CNCs in PP.

SSSP melt-state compression molding of the mechanical test samples.

Fig. 3 compares the change in Young's modulus observed with LDPE/CNC composites using SSSP, MM (in this study), and values reported by Dufresne and coworkers using TSE. Dufresne and co-workers [82] reported 6% and 24% increases in Young's modulus relative to that of neat LDPE for composites with 5 wt% and 10 wt% pristine CNC, respectively. These values compare well with a 13% increase observed in 90/10 wt% LDPE/CNC composites prepared using a miniMax molder in this study. In comparison, dramatically improved modulus values are observed in LDPE/CNC composites prepared by SSSP (38% for 5 wt% CNC and 69% for 10 wt% CNC). Additionally, it should be noted that the LDPE used in our study is twice as stiff as the one used in Ref. [82], with a modulus of 160 MPa. Additionally, these enhancements compare favorably with a 60% increase in modulus seen with incorporation of up to 9 wt% 1.0×10^6 g/mol PEO-wrapped-CNC in LDPE [87].

As shown in Fig. 4, the most dramatic deterioration in the mechanical properties of polyolefin/CNC composites made by MM is in elongation at break. For melt-mixed samples, elongation at break decreases from 510% for neat LDPE to 20% for the 90/10 wt% LDPE/CNC composite. Poor outcomes for elongation at break were also reported in literature studies for LDPE/CNC composites made by conventional TSE [82]. For example at 5 and 10 wt% CNC content, elongation at break was reported in Ref. [82] to be 50% and 5%, respectively, factors of 4 and 40 times smaller than that of the neat LDPE. In contrast, SSSP-processed LDPE/CNC composites retain elongation at break equal to that of neat polymer for CNC loadings up to 7 wt% and nearly equal for 10 wt% CNC loading. The superior dispersion achieved by SSSP with suppressed degradation during short-time post-SSSP compression molding of samples gives rise to such dramatic property enhancements.

In the case of 90/10 wt% PP/CNC composites prepared by MM, a maximum elongation at break of 7% is observed with brittle fracture (no yield point). For SSSP-processed 90/10 wt% PP/CNC composites, we observe major reduction in elongation at break to 12%, but due to the dramatically improved dispersion of CNC within the polymer matrix, the samples exhibit ductile behavior. The post-SSSP compression molding at 180 °C could cause minor CNC degradation, and loss of small molecules could explain the reduction in elongation at break [35]. Alternatively, the formation of a percolated network within the PP matrix could also lead to such reduction in elongation at break values. Similar behavior has been reported with PP/graphite nanocomposites prepared by SSSP [19]. It should be noted that PP employed in this study has elongation at yield of 10%. All PP/CNC composites produced by SSSP show ductile tensile response with elongation at break greater than 10%.

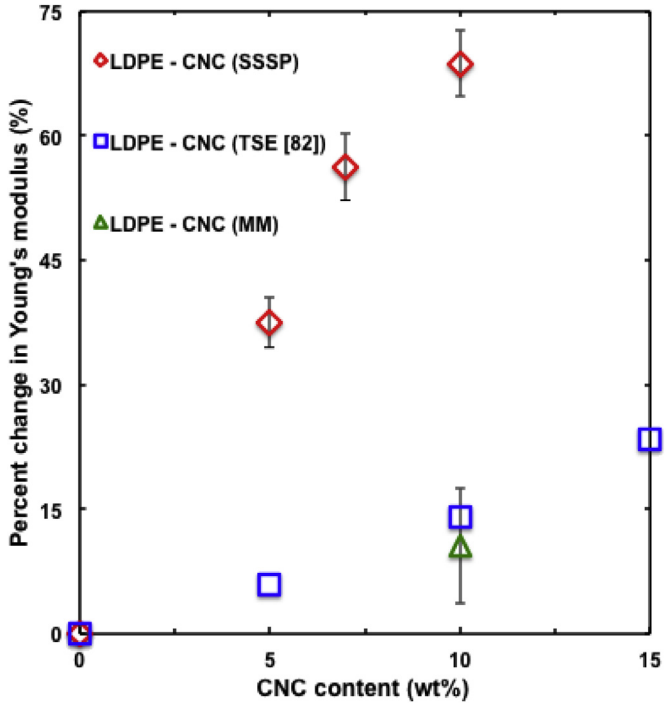

Fig. 3. Comparison of percent increase in Young's modulus of LDPE/CNC composites made by SSSP (diamond) with those made by MM (triangle; this study) and twin-screw extrusion (square; Ref. [82]). (Note: Neat LDPE had Young's modulus of 160 MPa in our study and 85 MPa in Ref. [82].)

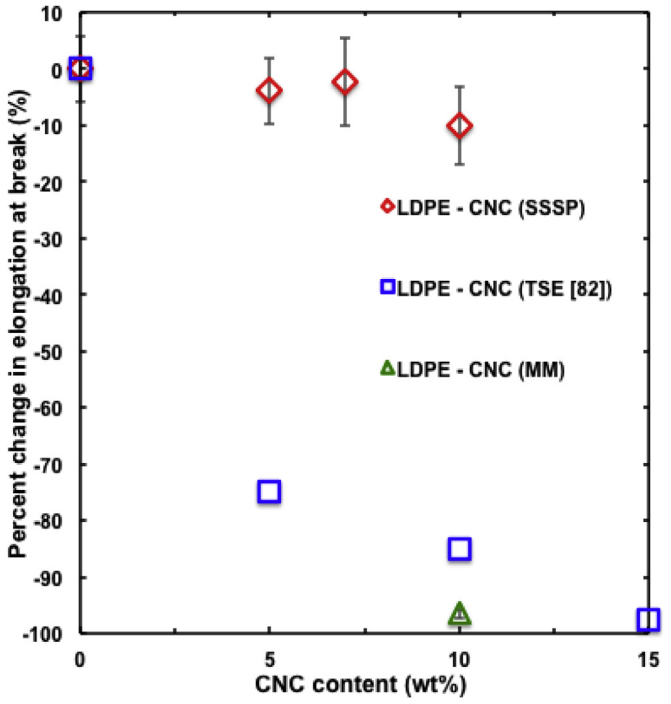

Fig. 4. Comparison of percent change in elongation at break of LDPE/CNC composites made by SSSP (diamond) with those made by MM (triangle; this study) and twin-screw extrusion (square; Ref. [82]). (Note: Neat LDPE had elongation at break of 510% in our study and 200% in Ref. [82].)

To the best of our knowledge, there are no studies reporting mechanical properties of PP/CNC composites prepared by TSE or other conventional melt processing techniques where solvent processing is not used first. Ljungberg et al. [75] employed solution processing to prepare composites of PP with pristine CNC. Nanocomposites reinforced with 6 wt% CNC displayed major reduction in both tensile strength and elongation at break. They observed brittle behavior with a 21% reduction in tensile strength. Comparatively, SSSP processed PP/CNC composites with 7 wt% CNC content exhibit 44% increase in Young's modulus and 8% increase in yield strength. Agarwal et al. [76] dissolved MAPP/CNC in toluene and PP. Upon solvent evaporation, the resulting powder was milled and blended in a lab-scale extruder into filaments. The modulus of the CNC composite was 17% higher than PP at a loading of 2 wt% with poor dispersion. In another study, Bahar et al. [77] incorporated 10 wt% CNC in PP using 2 wt% maleic anhydride as compatibilizer. Comparing to a control PP sample with the same maleic anhydride content, there was a 43% reduction in modulus for the composite. Properties reported for PP/CNC composites in those studies cannot rival those made by SSSP (~53% increase in Young's modulus with ductile yielding).

In summary, SSSP allows for the successful production of polyolefin/CNC composites with major improvements in Young's modulus (highest enhancements reported so far in the literature) and yield strength, and with retention of ductility. These properties can be achieved by SSSP processing without any chemical modification of CNC to enhance interfacial interactions. Chemical modification adopted in literature studies [75,77,82,87] has been suggested as key in improving adhesion between the hydrophobic PP matrix and the hydrophilic CNC filler. However, our results indicate that achieving optimal dispersion may be more important than achieving optimal interfacial interactions in the preparation of polyolefin/CNC composites.

3.1.2. *Mechanical properties of polyolefin/CNC composite – creep*

Time-dependent deformation or creep resulting from the application of a constant stress at constant temperature may determine the final application of polyolefin/CNC composites. Polymeric creep occurs due to a combination of elastic deformation and viscous flow. The creep response of composites is strongly dependent on stress levels, temperature and filler dispersion. As time progresses, the creep deformation may exceed the limit for structural failure of the composite. Hence, creep deformation must be taken into account when employing composites for structural applications. Further, it is imperative to measure and understand the creep response of such composites for their application in the automobile or construction industries [40,115].

Incorporation of fillers sometimes adds a more solid-like response that leads to reduced creep deformation [40,115–119]. Fig. 5 shows fractional displacement (or deformation) of SSSP-processed LDPE/CNC and PP/CNC composites as a function of time. Creep measurements were performed at a stress level of 50% of yield strength measured from tensile test experiments. At this stress level, neat LDPE and PP exhibit nonlinear deformation with time. At 30 min, neat LDPE has a creep deformation of 29%, while incorporation of well-dispersed CNC by SSSP leads to 25% and 17% creep deformation for 5 and 10 wt% CNC loading, respectively (Fig. 5a). At 30 min, neat PP exhibits a creep deformation of 48%; incorporating 5 and 10 wt% CNC by SSSP into the matrix reduces creep deformation to 31% and 27%, respectively. The excellent dispersion of CNC in the composites by SSSP can dramatically improve the effectiveness of stress transfer between polymer and filler in the absence of favorable thermodynamics, which in turn enhances the creep performance of such composites.

Table 3
Crystallization behavior of neat PP and PP/CNC composites prepared by SSSP.

Specimen	Nonisothermal onset crystallization temperature T_c (°C)	Isothermal crystallization half time at 140 °C $\tau_{1/2}$ (min)	Crystallinity X_c (%)
Neat LDPE Pellet[a]	97	–	30
95/5 wt% LDPE/CNC	98	–	32
93/7 wt% LDPE/CNC	98	–	32
90/10 wt% LDPE/CNC	98	–	32
Neat PP Pellet	121	54	52
95/5 wt% PP/CNC	128	26	56
93/7 wt% PP/CNC	128	20	55
90/10 wt% PP/CNC	129	13	56

[a] The LDPE used in this study exhibited extremely rapid crystallization, and no isothermal characterization was undertaken.

3.2. *Effect of CNC dispersion on crystallization behavior*

Further evidence of good filler dispersion in SSSP-processed composites can be seen via crystallization. Table 3 summarizes crystallization behavior of LDPE/CNC and PP/CNC composites prepared by SSSP. It should be noted that the LDPE employed in this study has extremely fast crystallization rates and does not, within error, show any further improvement in onset crystallization temperature ($T_{c,onset}$) or crystallinity upon CNC addition. Additionally, due to the fast rates of crystallization of LDPE, isothermal crystallization studies were not carried out. Results for PP/CNC indicates that the $T_{c,onset}$ value increases by 7–8 °C for 5 to 10 wt % CNC loadings in composites prepared by SSSP. This behavior is consistent with values reported by Ljungberg et al. [75] for PP/CNC composites prepared via solution processing and arises from the fact that the PP-filler interface serves as a site for heterogenous nucleation of crystals [34,35,75]. However, in another study by Bahar et al. [77] PP/CNC composites prepared by solution processing showed no change in $T_{c,onset}$. All PP/CNC composites prepared via SSSP exhibit slight increases in PP crystallinity relative to that of neat PP.

Fig. 6 shows nonisothermal crystallization curves (data summarized in Table 3) obtained at 10 °C/min cooling rates from the melt for neat PP and 90/10 wt% PP/CNC composite produced via SSSP. The DSC thermogram demonstrates a shift in crystallization onset and peak temperatures to higher temperature in the composite. Additionally, the PP/CNC composite exhibits the presence of double crystallization peaks. Ljungberg et al. [75] observed a similar

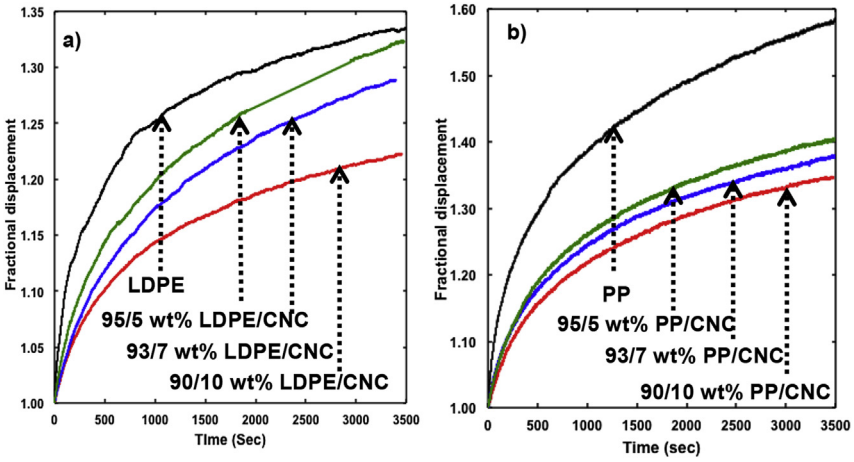

Fig. 5. Comparison of creep curves of neat polymer and polymer composites made by SSSP: a) neat LDPE and LDPE/CNC composites and b) neat PP and PP/CNC composites.

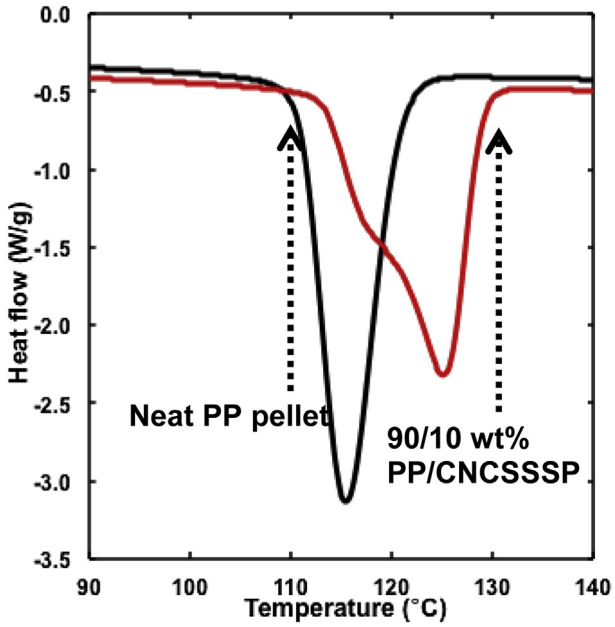

Fig. 6. Nonisothermal crystallization curves (10 °C/min cooling rate) for neat PP pellet and 90/10 wt% PP/CNC made by SSSP.

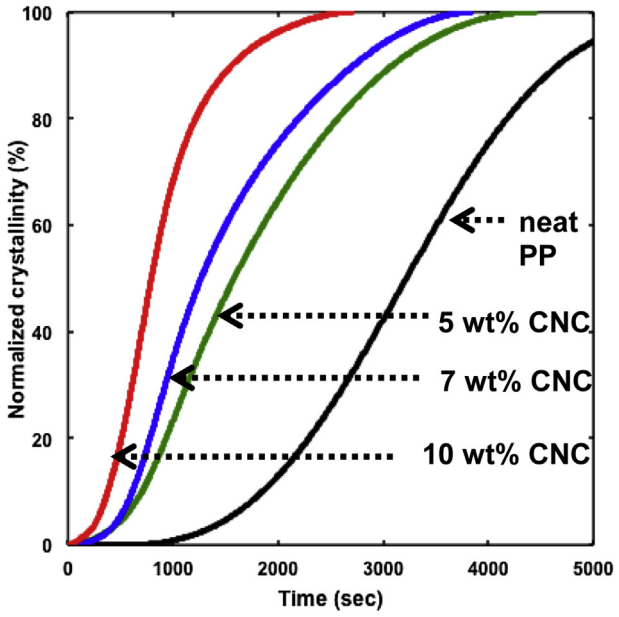

Fig. 7. Isothermal crystallization curves (140 °C) for neat PP and PP/CNC composites made by SSSP with different CNC contents. (Note: Normalized crystallinity is relative to crystallinity after 10800 s at 140 °C.)

double crystallization peak in their study, which they explained based on the possibility of CNC acting as a β nucleating agent for PP. Quantitative agreement was observed from x-ray diffraction data provided in their study. If the β crystal phase is present in the SSSP-processed composite, that may explain the lower elongation to failure in the composites as the β crystal phase is known to decrease ductility post yield [124]. However, differences in sample preparation for the two methods make it difficult to draw a direct comparison. A double crystallization peak could also arise from regions of composites that are lean and rich in CNC despite excellent dispersion. These observations are also consistent with results reported by Masuda et al. [14] in PP/carbon nanotube composites prepared by SSSP.

Isothermal crystallization curves measured by DSC at 140 °C are shown in Fig. 7. Isothermal crystallization half-times are recorded in Table 3. Neat PP had an isothermal crystallization half-time, $\tau_{1/2}$, of 54 min. Incorporation of CNC in PP reduces $\tau_{1/2}$ to 26 min and 13 min for 5 and 10 wt% CNC loadings. The symmetric nature of the crystallization–time curves indicates homogenous dispersion of CNC within the polymer. Thus, crystallization half-times coupled with the nature of the crystallization–time curves indicate the superior dispersion of CNC achieved by SSSP. It is also important to note that the extremely rapid crystallizability of such composites prepared by SSSP could dramatically reduce the cycle times in post-SSSP injection molding steps employed for producing final products.

3.3. Thermal degradation behavior of polyolefin/CNC composites in air and in nitrogen

Thermal degradation behavior is examined using a thermogravimetric analyzer in which samples are heated to 700 °C at a rate of 10 °C/min under both nitrogen and air atmospheres. Unlike other nanofillers such as carbon nanotubes or graphite that do not degrade under these conditions, CNCs undergo thermal degradation [14,19,78,79]. This makes quantitative analysis of filler content from final ash remaining at 700 °C impossible. In addition, similar to polymers, CNCs undergo degradation via a free radical mechanism. Hence, we report thermal degradation behavior of the polyolefin/CNC composites and not of the pure polymer in the composite. The degradation trends of CNC, polyolefin/CNC and neat polyolefin are shown in Figs. 8 and 9, with $T_{5\%}$, $T_{10\%}$ and $T_{20\%}$ (degradation temperature corresponding to a certain percent of mass loss) and the final ash content summarized in Tables 4 and 5. It should be noted that $T_{5\%}$ demonstrates mass loss mostly associated with water desorption and sulfate end group degradation, while $T_{10\%}$ and $T_{20\%}$ provide information regarding a radical initiated degradation mechanism and the ability of char formed by filler to act as thermal stabilizing agent, respectively.

Figs. 8 and 9 show that CNC undergoes a slow degradation process with ~2% mass loss at temperatures less than 120 °C in both nitrogen and air atmospheres. This initial mass loss at lower temperature is a result of moisture desorption from CNC due to its hydrophilic nature [78,79]. Upon further elevation in temperature, CNC exhibits an additional 1–2 % mass loss under 200 °C in an oxidative atmosphere. This mass loss is related to the elimination of sulfate end groups left behind from CNC preparation, which could subsequently catalyze β-elimination of hydroxyl groups on the cellulose ring structure [78,79]. At 253 °C, CNC suffers a total of 5% mass loss due to auto-oxidation of cellulose involving peroxide groups. On the other hand, under an inert nitrogen atmosphere, CNC show a gradual degradation behavior with $T_{5\%}$ of 280 °C.

At temperatures above 250 °C, degradation of cellulose proceeds through a concurrent route of depolymerization, dehydration and decomposition of glucosyl units, leaving behind charred residue [78]. The corresponding $T_{10\%}$ and $T_{20\%}$ for CNC occur at temperatures of 288 and 308 °C in nitrogen and at 265 and 277 °C in air. In nitrogen, CNC develops a slow charring process, leaving behind ~18% char as compared to ~5% in air at 700 °C. This difference is consistent with the oxidative gasification of charred residue. In addition to lowering degradation temperature, sulfate end groups from acid hydrolysis promote char formation in CNC, and the large amount of char produced makes CNC a candidate for flame retardant applications [79].

In nitrogen, 90/10 wt% LDPE/CNC composites undergo a 5% mass loss at 311 °C, which compares to 426 °C for neat LDPE. Relative to

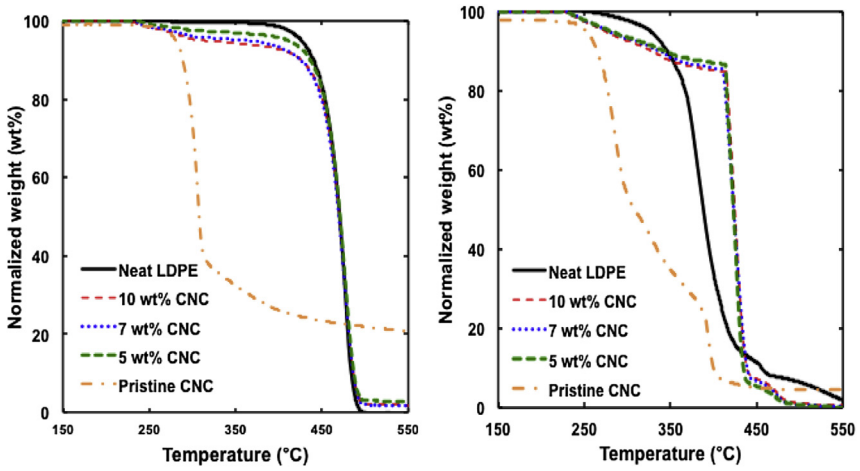

Fig. 8. Thermal degradation behavior of neat LDPE, CNC and LDPE/CNC composites made by SSSP with different CNC contents in nitrogen (left) and air (right).

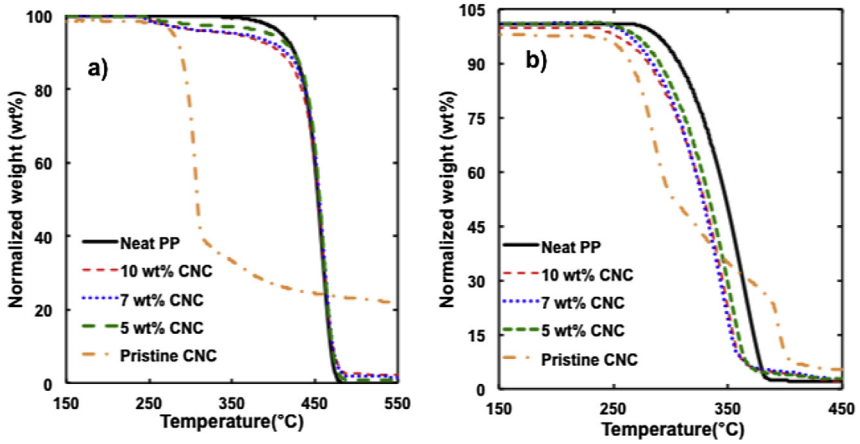

Fig. 9. Thermal degradation behavior of neat PP, CNC and PP/CNC composites made by SSSP with different CNC contents in a) nitrogen and b) air.

neat LDPE, incorporation of CNC in LDPE via SSSP results in the reduction of $T_{10\%}$ by 3 °C and 14 °C, respectively, for composites with 5 and 10 wt% CNC. The deterioration in the overall degradation behavior of the composite is consistent with CNC degradation at low temperature as explained previously. At higher temperature, char residue is produced that could provide a barrier to degradation. However, $T_{20\%}$ of 450–453 °C for CNC composites, similar to that of neat LDPE, indicates that char formed by CNC fails to improve thermal stability for the composite. The final residue left in the composite increases from 0.9 to 1.8 % (final mass percent) as filler loading increases from 5 to 10 wt%.

Under air atmosphere, LDPE undergoes thermoxidative degradation through a peroxide radical mechanism, with $T_{10\%}$ and $T_{20\%}$ of 346 and 367 °C, respectively [122,123]. The CNC undergoes degradation via a similar radical mechanism, and the LDPE composites with 5 and 10 wt% CNC content show dramatic reductions in $T_{5\%}$ of 46 and 55 °C, respectively, compared to neat LDPE. In contrast, $T_{10\%}$

Table 4
Thermal degradation behavior in nitrogen and air atmospheres of neat LDPE, LDPE/CNC composites made by SSSP, and CNC.

Specimen	$T_{5\%}$ (°C)	$T_{10\%}$ (°C)	$T_{20\%}$ (°C)	Ash[a] (%)
Nitrogen				
Neat LDPE pellet	426	440	453	–
95/5 wt% LDPE/CNC	410	437	453	0.9
93/7 wt% LDPE/CNC	359	425	450	1.2
90/10 wt% LDPE/CNC	311	426	451	1.8
CNC	280	288	308	18
Air				
Neat LDPE pellet	327	346	367	–
95/5 wt% LDPE/CNC	281	343	415	–
93/7 wt% LDPE/CNC	278	336	413	0.1
90/10 wt% LDPE/CNC	272	328	417	0.5
CNC	253	265	277	4.5

[a] Ash content is reported at 700 °C in both air and nitrogen.

Table 5
Thermal degradation behavior in nitrogen and air atmospheres of neat PP, PP/CNC composites made by SSSP, and CNC.

Specimen	$T_{5\%}$ (°C)	$T_{10\%}$ (°C)	$T_{20\%}$ (°C)	Ash (%)
Nitrogen				
Neat PP pellet	411	425	438	–
95/5 wt% PP/CNC	361	416	438	1.0
93/7 wt% PP/CNC	357	424	440	1.2
90/10 wt% PP/CNC	352	408	434	1.7
CNC	280	288	308	18
Air				
Neat PP pellet	297	307	323	1.7
95/5 wt% PP/CNC	277	291	306	2.0
93/7 wt% PP/CNC	273	288	304	2.1
90/10 wt% PP/CNC	266	281	299	1.0
CNC	253	265	277	4.5

shows a maximum 18 °C decrease compared to $T_{10\%}$ of neat LDPE, and $T_{20\%}$ exhibits a qualitatively different response with a 50 °C increase for the composites relative to neat LDPE. The mass loss in LDPE/CNC composites at lower temperatures is consistent with CNC degradation. We hypothesize that CNC, which is more susceptible to oxidative degradation at higher temperature, could undergo degradation preferentially and thus delay neat LDPE degradation. Similar observations have been made for composites of polyolefins with other cellulosic fillers [40,120,121].

Neat PP is more stable in nitrogen with higher $T_{10\%}$ and $T_{20\%}$ of 425 and 438 °C. Similar to LDPE/CNC composites, PP/CNC composites exhibit a decrease in $T_{5\%}$ of 50 and 59 °C, compared to that of neat PP, for 5 and 10 wt% filler content. The PP/CNC composites exhibit 9 and 17 °C reductions in $T_{10\%}$ for 5 and 10 wt% CNC, respectively, while $T_{20\%}$ of both composites is nearly invariant from that of neat PP. The relatively small decrease in degradation temperatures for higher percent mass loss indicates that under inert conditions, CNC undergoes low-temperature degradation without catalyzing degradation of the PP matrix. Thus, the relatively small change in $T_{20\%}$ temperatures indicates that the char formed by CNC does not improve thermal stability of the composites. In addition, the final char left at 700 °C qualitatively agrees with the increasing filler content in these composites.

In air, PP is more vulnerable to thermo-oxidative degradation compared to LDPE [122,123] and shows lower $T_{10\%}$ and $T_{20\%}$ of 307 and 323 °C. Addition of CNC reduces $T_{5\%}$ from 297 °C for neat PP to 277 °C for 95/5 wt% PP/CNC composite and 266 °C for 90/10 wt% PP/CNC composite. Comparing to neat PP, $T_{10\%}$ decreases by 16 °C for composites with 5 wt% CNC and by 26 °C with 10 wt% CNC, while $T_{20\%}$ decreases by 17 and 24 °C in composites with 5 and 10 wt% CNC, respectively. It is interesting to note that $T_{5\%}$ decreases by 46–55 °C for LDPE/CNC composites compared to 20–31 °C for PP/CNC. The less dramatic decreases in $T_{10\%}$ and $T_{20\%}$ relative to the reduction in $T_{5\%}$ for PP/CNC composites indicate that, unlike LDPE/CNC composites, CNC may undergo simultaneous degradation with PP.

As discussed previously, typical polyolefin melt processing conditions result in major CNC degradation so that composites show no improvement in mechanical properties. Similar observations have been made with cellulose-rich natural-fiber-reinforced composites [28]. Alternatively, SSSP provides an effective near-ambient-temperature processing route for producing polyolefin/CNC composites with excellent filler dispersion and no degradation during processing. (In contrast, melt mixing leads to poor CNC dispersion and degradation where CNC is present in the composite. Evidence of both the poor dispersion and reduced thermal stability of the polyolefin/CNC composites made by melt mixing is given in Supplementary Information.) In the next section, we will address how SSSP-processed composites perform under further melt processing to produce final products.

3.4. Post-SSSP melt processing of PP/CNC composites by single-screw extrusion

In order to understand the behavior of 90/10 wt% PP/CNC composites during post-SSSP melt processing, the SSSP-processed powder was further processed using single-screw extrusion (SSE). (High MFI PP, 9 g/10 min, was employed in this part of our study so that samples retain sufficiently low viscosity for extrusion at the low temperature of 175 °C.) In order to understand the effect of degradation, all zones were maintained at the same temperature during SSE. Composite samples were extruded with a short residence time of ~1 min.

Fig. 10 shows micrographs of PP/CNC composites extruded at different temperatures and the corresponding Young's moduli.

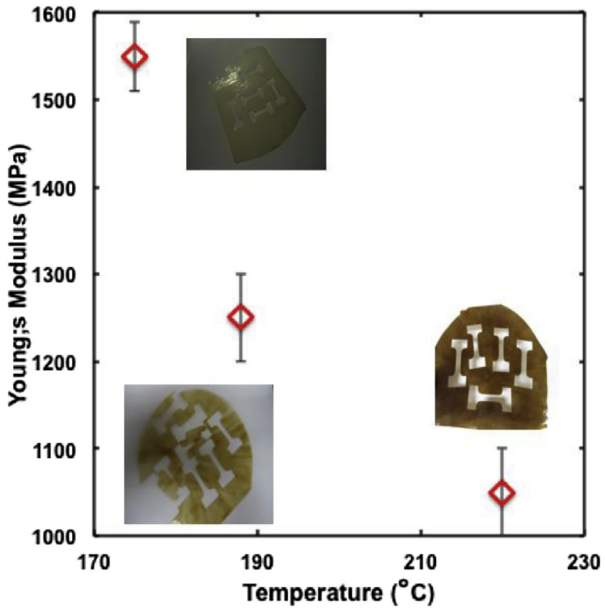

Fig. 10. Young's modulus and visual appearance of 95/5 wt% PP/CNC composites made by SSSP as a function of post-SSSP single-screw extrusion temperature. (Note. Neat PP used in these measurements had a Young's modulus of 1050 ± 30 MPa).

Composite samples turn from a uniform tan color to a more brown color when SSE temperature is raised from 175 °C to 220 °C. This behavior is consistent with the low temperature degradation of CNC observed from thermogravimetric analysis. Even for the short melt extrusion residence time employed here, CNC in the composite undergoes significant degradation at higher SSE temperatures.

The high MFI PP employed in this part of our study had Young's modulus of 1050 MPa. Incorporation of 10 wt% CNC via SSSP results in a ~48% increase in Young's modulus (the low MFI PP employed in previous sections showed a 53% increase in Young's modulus with 10 wt% CNC incorporation). The Young's modulus of the PP/CNC composites decreases with increasing extrusion temperature, from 1550 MPa to 1075 MPa (within error, identical to that of the neat PP) for extrusion temperatures ranging from 175 °C to 220 °C. The high temperature degradation of CNC could potentially destroy the crystalline structure of CNC resulting in no enhancement in Young's modulus for composites processed at high temperature.

Joseph et al. [28] reported the effect of mixing time and temperature on mechanical properties of PP/sisal composites prepared by TSE. They found that Young's modulus decreased with long mixing times at 170 °C, and a similar decrease was observed with increasing mixing temperature. They attributed this decrease to fiber size reduction and degradation. Increasing temperature during SSE results in major CNC degradation and thereby poor visual appearance of composite films and reduced mechanical properties. Hence, care must be taken during subsequent melt processing of SSSP-produced PP/CNC composite materials to suppress CNC degradation by appropriate selection of the melt processing temperature and residence time.

4. Conclusions

Solid-state shear pulverization is employed for the first time to produce polyolefin/CNC composites with 5–10 wt% unmodified CNC. Relative to composites made by melt mixing, optical and electron microscopy reveals excellent dispersion and suppression of CNC degradation within the polymer. Major improvements in

crystallization rate provide further evidence of superior CNC dispersion achieved by SSSP. Composites exhibit maximum 69% and 53% increases in Young's modulus relative to neat LDPE and neat PP, respectively, the highest reported for such composites made with unmodified CNC. The SSSP-produced composites also exhibit superior creep performance with modest increments in yield strength compared to neat polymer. The LDPE composites retain elongation at break values equal or close to that of neat LDPE, while PP composites exhibit major reductions in elongation at break.

The thermal stability of pristine CNC, neat polymer, and composites is examined in detail by thermogravimetric analysis. At a 10 °C/min heating rate, unmodified CNC undergoes 5% mass loss at temperatures below 250 °C. Despite char formation at elevated temperature, both LDPE/CNC and PP/CNC composites show reduced thermal stability up to 10% mass loss relative to neat polymer under nitrogen atmosphere. Under air atmosphere, LDPE/CNC composites show a large decrease in $T_{5\%}$ relative to neat LDPE but a large increase in $T_{20\%}$. In contrast, PP/CNC composites show reduced thermal stability relative to neat PP under oxidative conditions for all mass loss temperatures. We hypothesize that CNC undergoes preferential thermo-oxidative degradation in LDPE composites and simultaneous thermo-oxidative degradation in the case of PP. Care must be taken to suppress CNC degradation during post-SSSP melt processing into final products. Single-screw extrusion of SSSP-processed PP/CNC composites reveals that such materials can be melt processed into final products with suppressed filler degradation by selecting appropriate extrusion temperature and residence time.

Acknowledgments

We thank Richard Reiner and Alan Rudie at the Forest Products Laboratory for collaboration regarding the CNC and also thank Total Petrochemicals and ExxonMobil for providing PP and LDPE, respectively. We acknowledge support from the Initiative for Sustainability and Energy at Northwestern University (ISEN), Northwestern University, and a Northwestern University Terminal Year Fellowship (to K.A.I.). This study made use of Central Facilities supported by the NSF-MRSEC program (Grant DMR-1121262) at Northwestern University.

Appendix A. Supplementary data

Supplementary data related to this article can be found online at http://dx.doi.org/10.1016/j.polymer.2014.11.017.

References

[1] Liang JZ, Li RKY. Polym Compos 1998;19:698–703.
[2] Faulkner DL, Schmidt RL. Polym Eng Sci 1977;17:657–65.
[3] Fu S-Y, Lauke B, Mäder E, Yue C-Y, Hu X. Compos Part A Appl Sci Manuf 2000;31:1117–25.
[4] Yui H, Wu G, Sano H, Sumita M, Kino K. Polymer 2006;47:3599–608.
[5] Mucha M, Marszalek J, Fidrych A. Polymer 2000;41:4137–42.
[6] Bastide S, Binda N, Crespy A. Compos Sci Technol 1998;3538:747–52.
[7] Hooper JJ, Paynter CD, Riley AM, Elton NJ, House JK, Austell S. Polymer 1992;33:5215–24.
[8] Usuki A, Kojima Y, Kawasumi M, Okada A, Fukushima Y, Kurauchi T, et al. J Mater Res 1993;8:1179–84.
[9] Giannelis EP. Adv Mater 1996;8:29–35.
[10] Paul DR, Robeson LM. Polymer 2008;49:3187–204.
[11] Alexandre M, Dubois P. Mater Sci Eng R Rep 2000;28:1–63.
[12] McNally T, Pötschke P, Halley P, Murphy M, Martin D, Bell SEJ, et al. Polymer 2005;46:8222–32.
[13] Ramanathan T, Liu H, Brinson LC. J Polym Sci Part B Polym Phys 2005;43:2269–79.
[14] Masuda J, Torkelson JM. Macromolecules 2008;41:5974–7.
[15] Wakabayashi K, Pierre C, Dikin DA, Ruoff RS, Ramanathan T, Brinson LC, et al. Macromolecules 2008;41:1905–8.
[16] Mu M, Walker AM, Torkelson JM, Winey KI. Polymer 2008;49:1332–7.
[17] Pujari S, Ramanathan T, Kasimatis K, Masuda J, Andrews R, Torkelson JM, et al. J Polym Sci Part B Polym Phys 2009;47:1426–36.
[18] Gopakumar TG, Page DJYS. Polym Eng Sci 2004;44:1162–9.
[19] Wakabayashi K, Brunner PJ, Masuda J, Hewlett SA, Torkelson JM. Polymer 2010;51:5525–31.
[20] Kalaitzidou K, Fukushima H, Drzal LT. Carbon N Y 2007;45:1446–52.
[21] Chen G-H, Wu D-J, Weng W-G, Yan W-L. J Appl Polym Sci 2001;82:2506–13.
[22] Wu CL, Zhang MQ, Rong MZ, Friedrich K. Compos Sci Technol 2005;65:635–45.
[23] Liu Y, Kontopoulou M. Polymer 2006;47:7731–9.
[24] Chan C-M, Wu J, Li J-X, Cheung Y-K. Polymer 2002;43:2981–92.
[25] Zuiderduin WCJ, Westzaan C, Huetink J, Gaymans RJ. Polymer 2003;44:261–75.
[26] Ober CK, Cheng SZD, Hammond PT, Muthukumar M, Reichmanis E, Wooley KL, et al. Macromolecules 2009;42:465–71.
[27] Arib RMN, Sapuan SM, Ahmad MMHM, Paridah MT, Zaman HMDK. Mater Des 2006;27:391–6.
[28] Joseph PV, Joseph K, Thomas S. Compos Sci Technol 1999;59:1625–40.
[29] Doan T-T-L, Gao S-L, Mäder E. Compos Sci Technol 2006;66:952–63.
[30] Gassan J, Bledzki AK. Compos Part A Appl Sci Manuf 1997;28:1001–5.
[31] Ichazo MN, Albano C, Gonzalez J, Perera R, Candal MV. Compos Struct 2001;54:207–14.
[32] Angles M, Salvado J, Dufresne A. J Appl Polym Sci 1999;74:1962–77.
[33] Yang H-S, Kim H-J, Son J, Park H-J, Lee B-J, Hwang T-S. Compos Struct 2004;63:305–12.
[34] Yang H-S, Kim H-J, Park H-J, Lee B-J, Hwang T-S. Compos Struct 2007;77:45–55.
[35] Karnani R, Krishnan M, Narayan R. Polym Eng Sci 1997;37:476–83.
[36] Liu W, Misra M, Askeland P, Drzal LT, Mohanty AK. Polymer 2005;46:2710–21.
[37] La Mantia FP, Morreale M. Compos Part A Appl Sci Manuf 2011;42:579–88.
[38] Mishra S, Mohanty AK, Drzal LT, Misra M, Hinrichsen G. Macromol Mater Eng 2004;289:955–74.
[39] Saheb DN, Jog JP. Adv Polym Technol 1999;18:351–63.
[40] Spoljaric S, Genovese A, Shanks RA. Compos Part A Appl Sci Manuf 2009;40:791–9.
[41] Qiu W, Zhang F, Endo T, Hirotsu T. J Appl Polym Sci 2003;87:337–45.
[42] Mathew AP, Oksman K, Sain M. J Appl Polym Sci 2005;97:2014–25.
[43] Ranby BG. Acta Chem Scand 1949;3:649–50.
[44] Ranby BG, Ribi E. Experientia 1950;6:12–4.
[45] Bondeson D, Mathew A, Oksman K. Cellulose 2006;13:171–80.
[46] Beck-Candanedo S, Roman M, Gray DG. Biomacromolecules 2005;6:1048–54.
[47] Saito T, Isogai A. Biomacromolecules 2004;5:1983–9.
[48] Saito T, Kimura S, Nishiyama Y, Isogai A. Biomacromolecules 2007;8:2485–91.
[49] Lavoine N, Desloges I, Dufresne A, Bras J. Carbohydr Polym 2012;90:735–64.
[50] Brinchi L, Cotana F, Fortunati E, Kenny JM. Carbohydr Polym 2013;94:154–69.
[51] Moon RJ, Martini A, Nairn J, Simonsen J, Youngblood J. Chem Soc Rev 2011;40:3941–94.
[52] Habibi Y, Lucia LA, Rojas OJ. Chem Rev 2010;110:3479–500.
[53] Mariano M, El Kissi N, Dufresne A. J Polym Sci Part B Polym Phys 2014;52:791–806.
[54] Diaz JA, Wu X, Martini A, Youngblood JP, Moon RJ. Biomacromolecules 2013;14:2900–8.
[55] Reising AB, Moon RJ, Youngblood JP. J Sci Technol For Prod Process 2012;2:32–41.
[56] Landry V, Alemdar A, Blanchet P. For Prod J 2011;61:104–12.
[57] Csoka L, Hoeger IC, Rojas OJ, Peszlen I, Pawlak JJ, Peralta PN. ACS Macro Lett 2012;1:867–70.
[58] Reiner RS, Rudie AW. Production and applications of cellulose nanomaterials. TAPPI PRESS; 2013.
[59] Mathew AP, Oksman K, Karim Z, Liu P, Khan SA, Naseri N. Ind Crops Prod 2014;58:212–9.
[60] Evans J. Manufacturing the carbon nanotube market. Chemistry world. RSC Publication; Nov 2007.
[61] Favier V, Canova GR, Cavaille JY, Chanzy H, Dufresne A, Gauthier C. Polym Adv Technol 1995;6:351–5.
[62] Siró I, Plackett D. Cellulose 2010;17:459–94.
[63] Eichhorn SJ. Soft Matter 2011;7:303.
[64] Eichhorn SJ, Dufresne A, Aranguren M, Marcovich NE, Capadona JR, Rowan SJ, et al. J Mater Sci 2009;45:1–33.
[65] Roohani M, Habibi Y, Belgacem NM, Ebrahim G, Karimi AN, Dufresne A. Eur Polym J 2008;44:2489–98.
[66] Peresin MS, Habibi Y, Zoppe JO, Pawlak JJ, Rojas OJ. Biomacromolecules 2010;11:674–81.
[67] Zhou C, Chu R, Wu R, Wu Q. Biomacromolecules 2011;12:2617–25.
[68] Anglès MN, Dufresne A. Macromolecules 2000;33:8344–53.
[69] Xu S, Girouard N, Schueneman G, Shofner ML, Meredith JC. Polymer 2013;54:6589–98.
[70] Dagnon KL, Shanmuganathan K, Weder C, Rowan SJ. Macromolecules 2012;45:4707–15.

[71] Pei A, Malho J-M, Ruokolainen J, Zhou Q, Berglund LA. Macromolecules 2011;44:4422–7.
[72] Heux L, Chauve G, Bonini C. Langmuir 2000;07493:8210–2.
[73] Kvien I, Tanem BS, Oksman K. Biomacromolecules 2005;6:3160–5.
[74] Iwatake A, Nogi M, Yano H. Compos Sci Technol 2008;68:2103–6.
[75] Ljungberg N, Cavaillé J-Y, Heux L. Polymer 2006;47:6285–92.
[76] Agarwal UP, Sabo R, Reiner RS, Clemons CM, Rudie AW. Appl Spectrosc 2012;66:750–6.
[77] Bahar E, Ucar N, Onen A, Wang Y, Oksuz M, Ayaz O, et al. J Appl Polym Sci 2012;125:2882–9.
[78] Wang N, Ding E, Cheng R. Polymer 2007;48:3486–93.
[79] Roman M, Winter WT. Biomacromolecules 2004;5:1671–7.
[80] Lin N, Chen G, Huang J, Dufresne A, Chang PR. J Appl Polym Sci 2009;113:3417–25.
[81] Oksman K, Mathew AP, Bondeson D, Kvien I. Compos Sci Technol 2006;66:2776–84.
[82] Junior de Menezes A, Siqueira G, Curvelo AS, Dufresne A. Polymer 2009;50:4552–63.
[83] Bondeson D, Oksman K. Compos Part A Appl Sci Manuf 2007;38:2486–92.
[84] Goffin AL, Raquez J-M, Duquesne E, Siqueira G, Habibi Y, Dufresne A, et al. Polymer 2011;52:1532–8.
[85] Ben Azouz K, Ramires EC, Van den Fonteyne W, El Kissi N, Dufresne A. ACS Macro Lett 2012;1:236–40.
[86] Lin N, Dufresne A. Macromolecules 2013;46:5570–83.
[87] Pereda M, El Kissi N, Dufresne A. ACS Appl Mater Interfaces 2014;6:9365–75.
[88] Corrêa AC, Morais Teixeira E, Carmona VB, Teodoro KBR, Ribeiro C, Mattoso LHC, et al. Cellulose 2013;21:311–22.
[89] Torkelson JM, Lebovitz AH, Kasimatis K, Khait K. US patent 2007; 20080176980-A1.
[90] Jiang X, Drzal LT. J Appl Polym Sci 2012;124:525–35.
[91] Lebovitz AH, Khait K, Torkelson JM. Polymer 2003;44:199–206.
[92] Tao Y, Kim J, Torkelson JM. Polymer 2006;47:6773–81.
[93] Tao Y, Lebovitz AH, Torkelson JM. Polymer 2005;46:4753–61.
[94] Furgiuele N, Lebovitz AH, Khait K, Torkelson JM. Macromolecules 2000;33:225–8.
[95] Lebovitz AH, Khait K, Torkelson JM. Macromolecules 2002;35:8672–5.
[96] Diop MF, Burghardt WR, Torkelson JM. Polymer 2014;55:4948–58.
[97] Iwamoto S, Yamamoto S, Lee S-H, Endo T. Cellulose 2014;21:1573–80.
[98] Walker A, Tao Y, Torkelson J. Polymer 2007;48:1066–74.
[99] Iyer KA, Torkelson JM. Polym Compos 2013;34:1211–21.
[100] Iyer KA, Torkelson JM. Compos Sci Technol 2014;102:152–60.
[101] Diop MF, Torkelson JM. Polymer 2013;54:4143–54.
[102] Diop MF, Torkelson JM. Macromolecules 2013;46:7834–44.
[103] Brunner PJ, Clark JT, Torkelson JM, Wakabayashi K. Polym Eng Sci 2012;52:1555–64.
[104] Guo W, Chen G. J Appl Polym Sci 2014;131:1–5.
[105] Sorrentino A, Gorrasi G, Tortora M, Vittoria V, Costantino U, Marmottini F, et al. Polymer 2005;46:1601–8.
[106] Xia H, Wang Q, Li K, Hu G-H. J Appl Polym Sci 2004;93:378–86.
[107] Saito T, Okamoto M. Polymer 2010;51:4238–42.
[108] Tang L, Wan Y, Yan D, Pei Y, Zhao L, Li Y. Carbon N Y 2013;60:16–27.
[109] Wu H, Sun X, Zhang W, Zhang X, Lu C. Compos Part A Appl Sci Manuf 2013;55:27–34.
[110] Wu H, Rook B, Drzal LT. Polym Compos 2013;34:426–32.
[111] Perrin-Sarazin F, Sepehr M, Bouaricha S, Denault J. Polym Eng Sci 2009;49:651–65.
[112] Maric M, Macosko CW. Polym Eng Sci 2001;41:118–30.
[113] Bu H-S, Cheng SZD, Wunderlich B. Makromol Chem Rapid Commun 1988;9:75–7.
[114] Wunderlich B. Macromolecular physics, vol. 3. New York: Academic Press; 1980.
[115] Ashori A. Bioresour Technol 2008;99:4661–7.
[116] Bledzki AK, Faruk O. Compos Sci Technol 2004;64:693–700.
[117] Bengtsson M, Gatenholm P, Oksman K. Compos Sci Technol 2005;65:1468–79.
[118] Lee S-Y, Yang H-S, Kim H-J, Jeong C-S, Lim B-S, Lee J-N. Compos Struct 2004;65:459–69.
[119] Sobczak L, Lang RW, Haider A. Compos Sci Technol 2012;72:550–7.
[120] Yang H-S, Wolcott MP, Kim H-S, Kim H-J. J Therm Anal Calorim 2005;82:157–60.
[121] Kim H-S, Kim S, Kim H-J, Yang H-S. Thermochim Acta 2006;451:181–8.
[122] Wong ACY, Lam F. Polym Test 2002;21:691–6.
[123] Peterson JD, Vyazovkin S, Wight CA. Macromol Chem Phys 2001;202:775–84.
[124] Shi G, Chu F, Zhou G, Han Z. Makromol Chem 1989;913:907–13.